Supplementary Information

Cobalt polyoxometalate-LDH hybrids: pH-switchable molecular catalysts to confined cobalt oxide oxygen evolution layers

Javier Quirós-Huerta,[a] Ramón Torres-Cavanillas,[a] Susana Ochando-Pariente,[a] Eugenio Coronado[a] and Joaquín Soriano-López *[a]

[a] Institut de Ciència Molecular, Universitat de València, Catedrático José Beltrán 2, 46980 Paterna, Spain.

Correspondence to: joaquin.soriano@uv.es

1) Instrumentation and Methodology:

Attenuated Total Reflectance Fourier-Transform Infrared (ATR-FTIR): Spectra were collected using an Agilent Cary 630 FTIR spectrometer in the 4000–350 cm^{-1} range.

Inductively Coupled-Plasma Mass Spectrometry (ICP-MS): The ICP-MS analyses were performed at the University of Valencia (Sección de Espectrometría Atómica y Molecular). The samples were digested in acid medium at 220 ºC using a microwave oven.

Transmission Electron Microscopy and Electron Diffraction X-ray Scattering (TEM and EDX): TEM images and EDX mapping were performed in a HRTEM TECNAI 200 kV microscope operating at 200 kV. The samples were prepared by dropping sample suspension in EtOH on lacey formvar/carbon copper grids (330 mesh).

Powder X-Ray Diffraction (PXRD): PXRD patterns were collected using a capillary with a PANalytical X'Pert diffractometer at room temperature using the copper radiation (Cu-Kα = 1.54178 Å) in the 2-70 degrees region.

Thermogravimetric Analysis (TGA): TGA measurements were carried out under N_2 atmosphere employing a TA instruments TGA 550 in the 25–700 °C temperature range with a temperature ramp of 10 °C/min.

X-ray Photoelectron Spectroscopy (XPS): XPS measurements were performed in an ultrahigh vacuum system ESCALAB210 (base pressure 1.0 × 10^{-10} mbar) from Thermo VG Scientific. Photoelectrons were excited by using the Mg Kα line (1253.6 eV). All spectra were referred to the Fermi level.

2) Materials and Synthetic Details:

All chemical reagents were used as purchased without further purification. Sodium tungstate dihydrate, cobalt nitrate hexahydrate, sodium phosphate dibasic, sodium phosphate monobasic monohydrate, potassium acetate, sodium chloride, sodium nitrate, bromine, magnesium chloride hexahydrate, urea, and hydrochloric acid were purchased from Sigma-Aldrich. Nafion™ D520 solution (~5%) was purchased from Ion Power. Cobalt acetate tetrahydrate and carbon black, acetylene 50% compressed were purchased from Alfa Aesar. Aluminum chloride hexahydrate, glacial acetic acid, and potassium hydroxide were purchased from Thermo Scientific Chemicals. Ethanol absolute and isopropanol were purchased from Scharlab. All the experiments were performed using milli-Q water, which was obtained from a Millipore Milli-Q equipment.

Synthesis of Mg_2Al-Cl-LDH (Mg_2Al-LDH): This LDH was prepared following the urea hydrolysis method under hydrothermal conditions. Firstly, 250 mM aqueous solutions of $MgCl_2{\cdot}6H_2O$ and $AlCl_3{\cdot}6H_2O$ were prepared separately. These stock solutions were stored at 4 °C. Next, 36 mL of the $MgCl_2$ solution, 18 mL of the $AlCl_3$ solution, and 36 mL of water were mixed in a Teflon vial, to which 2.365 g (39.4 mmol) of urea were added, and the resulting mixture was stirred for 5 minutes. Then, the hydrothermal reaction was conducted in an oven at 140 °C for 24 hours. After cooling down to room temperature, the Mg_2Al-LDH obtained was recovered by centrifugation and washed several times with water until the resulting washing waters had a neutral pH. At this point, it was washed with EtOH and dried under vacuum for 24 hours. The infra-red spectrum of the as-synthesized Mg_2Al-LDH indicates the presence of carbonate anions in the interlayer space of the LDH. Therefore, the carbonate anions had to be removed from the

structure by anion exchange. For this purpose, a 1M NaCl aqueous solution using 1 L of water was prepared in a round bottom flask and HCl was added until reaching a final concentration of 3.3 mM. Once this solution was deaerated with N_2, 1 g of the as-synthesized Mg_2Al-CO_3-LDH was added and left under stirring and under a flow of N_2 for 12 hours. Importantly, this anion exchange step was repeated twice to reduce as much as possible the presence of carbonate anions in the lamellar space of the LDH. Finally, the Mg_2Al-Cl-LDH was recovered by centrifugation, washed three times with water, then with EtOH, and dried under vacuum overnight.

Synthesis of $K_{16}[Co_9(H_2O)_6(OH)_3(HPO_4)_2(PW_9O_{34})_3]\cdot 63.9H_2O$ (Co_9): Co_9 was prepared as described in the literature.[1] $Na_2WO_4\cdot 2H_2O$ (33.00 g, 100.00 mmol) and Na_2HPO_4 (3.30 g, 22.00 mmol) were dissolved in 100 mL aqueous solution and the pH of the solution was adjusted to 7.1 by adding acetic acid. Thereafter, $Co(OOC\text{-}CH_3)_2\cdot 4H_2O$ (9.00 g, 35.00 mmol) was dissolved in 30 mL of water and then added to the previous solution. The resulting violet suspension was refluxed for 2 hours. After reflux, the hot solution was filtered and an excess of $K(OOC\text{-}CH_3)$ (2 g) was added. Then, the solution was filtered again, cooled down at room temperature, and stored to allow crystallisation of $K_{10}[Co_4(H_2O)_2(PW_9O_{34})_2]$ (Co_4) and $K_{16}[Co_9(H_2O)_6(OH)_3(HPO_4)_2(PW_9O_{34})_3]$. The latter was extracted with cold water, while Co_4 remained insoluble. The Co_9 solution was cooled at 4 °C and precipitated by adding $K(OOC\text{-}CH_3)$ in excess. The recovered precipitate was dissolved with cold water and precipitated again by adding $K(OOC\text{-}CH_3)$ in excess to remove any Co_4 impurities. This process was repeated several times to ensure that all the Co_4 is removed from the Co_9 precipitate. The pink precipitate was then recovered by filtration, washed with cold water, methanol, and acetone, and then dried under vacuum. Co_9 was characterized by FTIR (Fig. 1(b)), TGA (Fig. S1), ICP-MS (Table S1), and

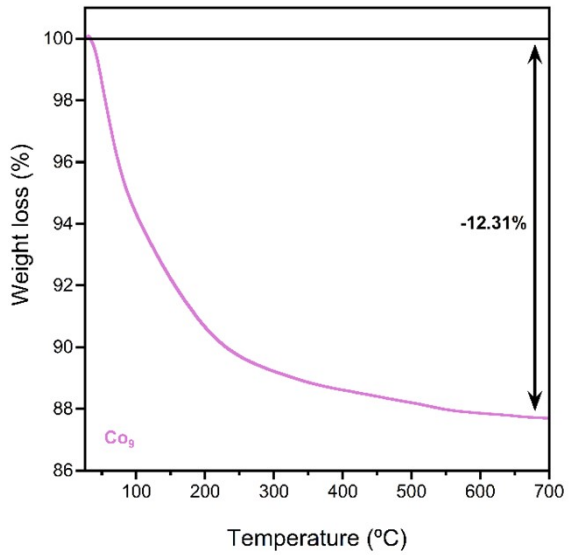

Fig. S1 Thermogravimetric analysis of the as-prepared Co_9 POM.

XPS (Fig. 2).

Synthesis of $Na_{16}[Co_4(H_2O)_2(P_2W_{15}O_{56})_2]\cdot 47.7H_2O$ (Co_4-WD): Co_4-WD was prepared as described in the literature.[2] $Co(NO_3)_2\cdot 6H_2O$ (0.73 g, 2.50 mmol) was dissolved in 50 mL of a 1M NaCl solution. Solid, freshly prepared $Na_{12}P_2W_{15}O_{56}$ (5.00 g, 1.25 mmol) was then added, and the solution was heated at 80 °C under stirring until the original light pink solution became a homogeneous red-brown solution that reflected green. Then, the solution was cooled at 5 °C

overnight. The crystalline green-brown solid was collected by filtration, washed with water and

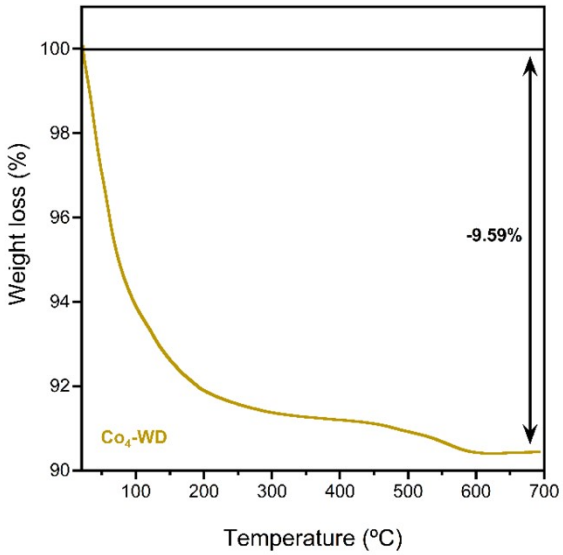

Fig. S2 Thermogravimetric analysis of the as-prepared Co_4-WD POM.

acetone, and dried at 80 °C under vacuum. Co_4-WD was characterized by FTIR (Fig. S3), TGA (Fig. S2), ICP-MS (Table S1), and XPS (Fig. 2).

Fabrication of the hybrid Co-POM/Mg_2Al nanocomposites: The hybrid nanocomposites were prepared following our recently reported protocol.[3] Mg_2Al-Cl-LDH (8.0 mg) and 4 mL of formamide were placed in a sealed vial and purged with Ar for 30 minutes. Then, the vial was sonicated in an ultrasound bath for 20 minutes. Once the LDH was dispersed, a 5 mM aqueous solution of the corresponding Co-POM (either Co_9 or Co_4WD), which was previously deaerated with Ar for 30 minutes, was added dropwise by piercing through the septum of the sealed vial using a syringe while stirring the LDH dispersion. Thereafter, the mixture was left under stirring for 20 hours in an Ar atmosphere. After this time, the hybrid nanocomposite was recovered by centrifugation, washed three times with water, then with EtOH, and finally, dried under vacuum overnight.

3) Electrochemical Procedures:

The electrochemical measurements were performed in Biologic VSP potentiostat employing a typical three-electrode set-up. As working electrodes for carrying out cyclic voltammetries (CV) and linear sweep voltammeteries (LSV) we used glassy carbon rotating disk electrodes (RDE-GC, 0.07 cm^2), carbon paper (CP, ca. 1 cm^2) was used for the chronoamperometries, and a rotating ring disk electrode (RRDE, 0.196 cm^2) consisting of a glassy carbon disk and a Pt ring was employed for O_2 detection. The set-up was completed by a Ag/AgCl (3M KCl) reference electrode and a Pt wire/mesh as counter electrodes. Two different buffered solutions were employed in this work: i) 0.1 M sodium phosphate (NaP_i) buffer at pH 6.9, containing 1M $NaNO_3$ as an electrolyte; and ii) 1 M KOH at pH 14.2. The ohmic drop (iR) was compensated (85%) using the positive feedback as implemented in the potentiostat by performing current interrupt measurements prior to each experiment. Note that for the RRDE experiments working in bipotentiostat mode, the iR drop was not compensated. The buffer solutions were degassed with Ar for at least 30 minutes before each experiment. Before conducting the LSV measurements, CV at a scan rate of 100 mV/s was performed as a preconditioning step of the

materials until no substantial changes were observed (typically 20 cycles). LSVs were performed at a scan rate of 1 mV/s and at a rotation of 1600 rpm (700 rpm for RRDE experiments), which was controlled with an Autolab RDE motor controller. LSV data was used for Tafel analyses. Chronoamperometry measurements were carried out in an H-cell where the working and reference electrodes were separated from the counter electrode by a glass frit (P0). For these experiments, the applied overpotentials were 700 mV and 500 mV when using NaP_i at pH 6.9, and KOH at pH 14.2, respectively. All the measurements were repeated at least three times to ensure reproducibility of the results.

The Nernst equation was employed to calculate the thermodynamic potential for the water oxidation ($E^{0}_{H_2O/O_2}$) at each pH used:

$$E^{0}_{H_2O/O_2} = 1.229 - (0.059 \times pH)(V)\ vs\ NHE\ at\ 25\ ^{\circ}C \quad \text{(Eq. S1)}$$

All applied potentials (E_{app}) were converted to the NHE reference scale using $E_{NHE} = E_{Ag/AgCl} + 0.210\ (V)$. The overpotentials were calculated by subtracting the thermodynamic water oxidation potential ($E^{0}_{H_2O/O_2}$) from E_{app} as:

$$\eta = E_{app} - E^{0}_{H_2O/O_2} \quad \text{(Eq. S2)}$$

The intrinsic catalytic activity was calculated based on the estimated electrochemical surface area (ECSA, cm^2). To this end, CVs were performed at ±50 mV vs open-circuit potential at different scan rates (50, 100, 150, 200, 300, 400, and 500 mV/s). The C_{dl} was calculated from ΔI ($I_a - I_c$) vs scan-rate plot, where the slope = 2 × C_{dl}. Anodic and cathodic current values were taken from the CVs at the open-circuit potential value. The estimated ECSA values were obtained by dividing C_{dl} by the specific capacitance (C_s) for which we took the commonly employed value of 40 µF/cm^2.[4] Thereafter, the roughness factor (R_F, dimensionless) was calculated by dividing the ECSA value by the geometrical area of the electrodes. Finally, the intrinsic current densities were calculated by dividing the current densities by the estimated R_F of each electrode.

The current densities were calculated based on the geometrical surface area of the electrodes. The obtained current densities were set to a value of 0 mA/cm^2 at 0 mV of overpotential. The onset potentials were estimated from the intersection point between the tangent lines of the Faradaic current at 0.2 mA/cm^2 and the non-Faradic current. Herein, all the potentials are given versus NHE, unless otherwise stated.

Electrolyte preparation: The 0.1 M sodium phosphate (NaP_i) buffer at pH 6.9, containing 1M $NaNO_3$ as an electrolyte, was prepared by dissolving 10.9877 g of Na_2HPO_4 and 3.1186 g of $NaH_2PO_4 \cdot H_2O$ in 500 mL of milli-Q water. Subsequently, 84.99 g of $NaNO_3$ was added, and the solution was diluted to a final volume of 1 L with milli-Q water.

The 1 M KOH electrolyte was prepared by dissolving 56.11 g of KOH in milli-Q water and diluting to a final volume of 1 L. The resulting solution had a measured pH of 14.2.

Electrode preparation: Nafion inks were prepared by dispersing 2mg of each sample and 1 mg of carbon black in 0.5 mL of a 1:1 (H_2O:EtOH) solution and 10 µL of a Nafion™ D520 solution (~5%). Then the mixture was sonicated for 2 hours to obtain a homogeneous suspension. Aliquots of 5 µL were drop-casted on the glassy carbon electrodes (already polished with 1.0

and 0.05 µm alumina powder) and dried at room temperature. For chronoamperometric measurements, we employed carbon paper electrodes. Pieces of 1 × 2 cm of carbon paper were cut and sonicated in HNO_3 for at least 2 hours to activate the surface. Then the electrodes were rinsed thoroughly with water and then with ethanol and dried under Ar flow. The electrode surface was masked with Kapton tape, leaving an active surface of approximately 1 × 1 cm (note that the real surface area for each electrode was measured and considered for the calculation of the current densities). Six aliquots of 10 µL (60 µL in total) of the corresponding Nafion ink

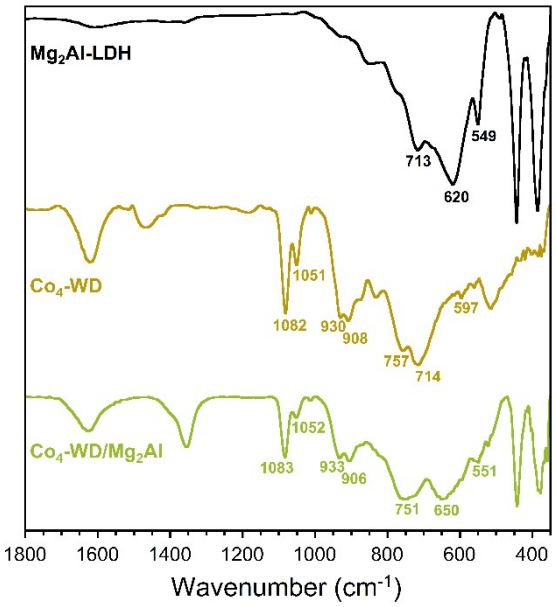

Fig. S3 FT-IR spectra of Mg_2Al-LDH, Co_4-WD POM, and Co_4-WD/Mg_2Al. Note that the peak shown at ca. 1360 cm^{-1} in the nanocomposites indicates the incorporation of carbonate anions during the Co-POM intercalation step.

were drop-cast on the carbon paper electrodes. Thereafter, the inks were dried at room temperature, followed by a drying step at 80 °C for at least 30 minutes. The electrodes were weighed before and after the deposition of the Nafion ink, resulting in a total mass deposited of ca. 0.3 mg in each electrode.

4) Characterisation:

Table S1: Elemental analysis (ICP-MS) of the fresh samples. For those containing Co-POMs, the data was normalized to the W content to facilitate the comparison. For Mg_2Al-LDH the data was normalized to the Mg content.

		Mg	Al	Co	W	P
Mg_2Al-LDH	mg/g	215	123.9	-	-	-
	µmols/g	8845.92	4591.95	-	-	-
	molar ratio	2.00	1.04	-	-	-
Co_9	mg/g	-	-	58.8	680	14.7
	µmols/g	-	-	997.74	3698.87	474.59
	molar ratio	-	-	7.28	27.00	3.46
Co_9/Mg_2Al	mg/g	63.5	35.6	46.6	571	12.1
	µmols/g	2612.63	1319.40	790.73	3105.96	390.65
	molar ratio	22.71	11.47	6.87	27.00	6.40
Co_4-WD	mg/g	-	-	25.79	791	11.31

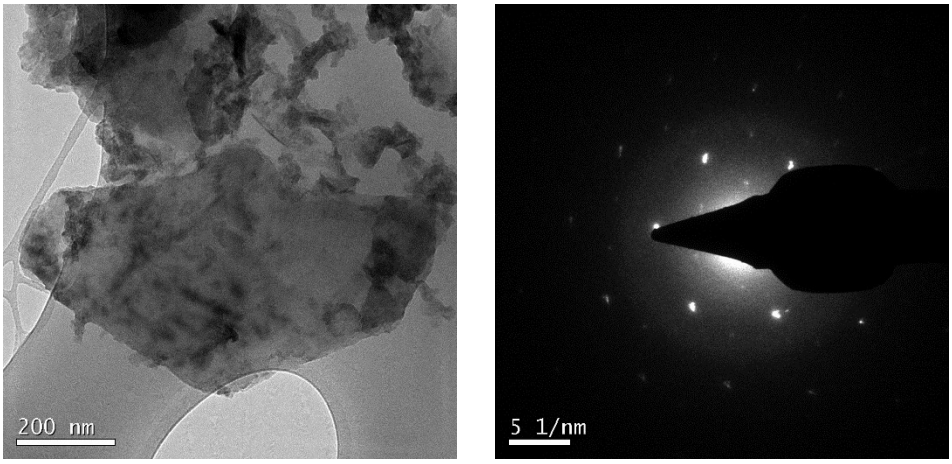

Fig. S4 Transmission electron microscopy image (left) and electron diffraction pattern (right) of the freshly prepared Co_9/Mg_2Al hybrid nanocomposite.

	µmols/g	-	-	437.62	4302.65	365.15
	molar ratio	-	-	3.05	30.00	2.55
Co_4-WD/Mg_2Al	mg/g	78.1	44.9	19.00	539	7.49
	µmols/g	3213.33	1664.07	322.40	2931.90	241.82
	molar ratio	32.88	17.03	3.30	30.00	2.47

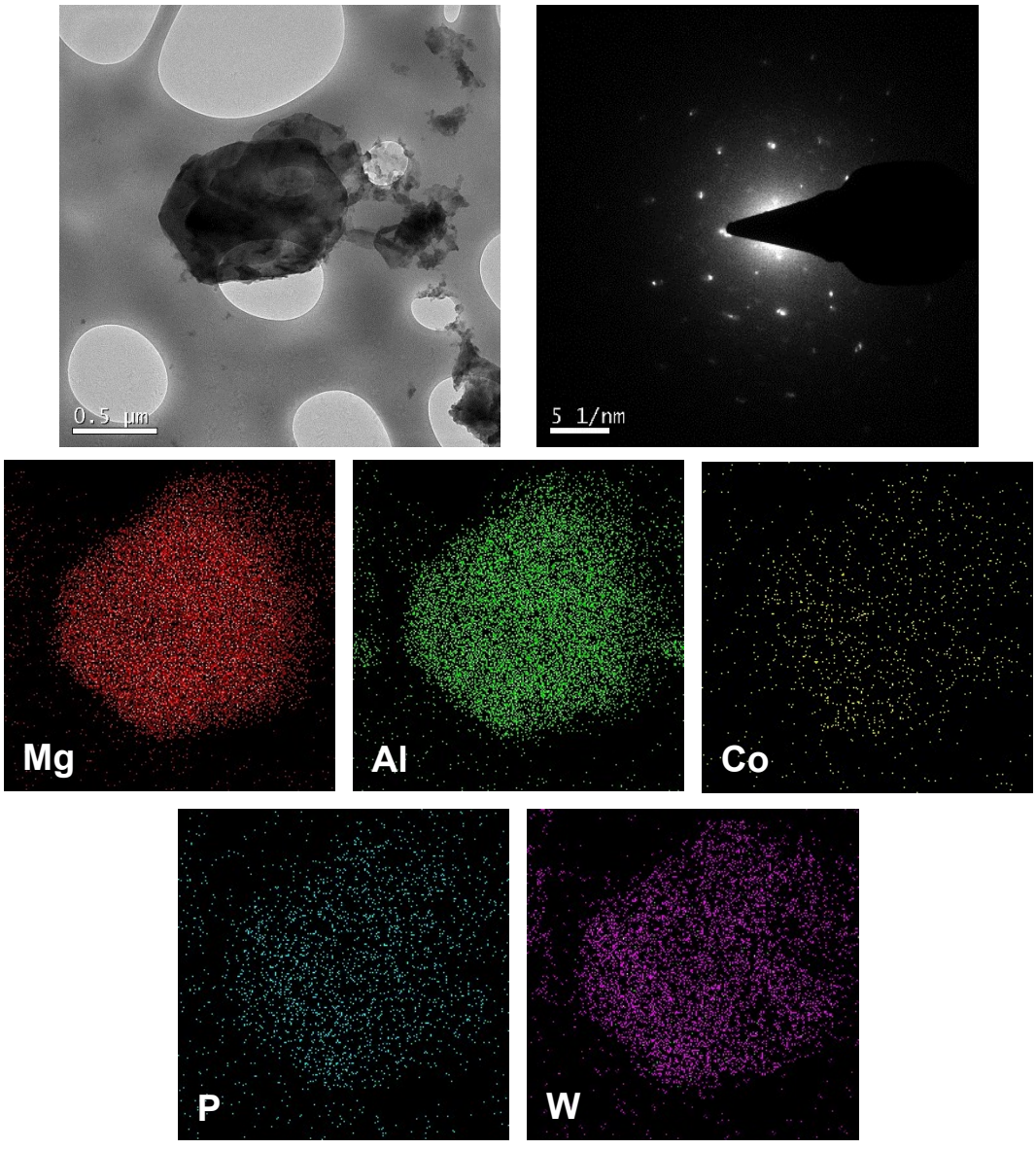

Fig. S5 Transmission electron microscopy image, electron diffraction pattern, and EDX elemental mapping of the freshly prepared Co_4-WD/Mg_2Al hybrid nanocomposite.

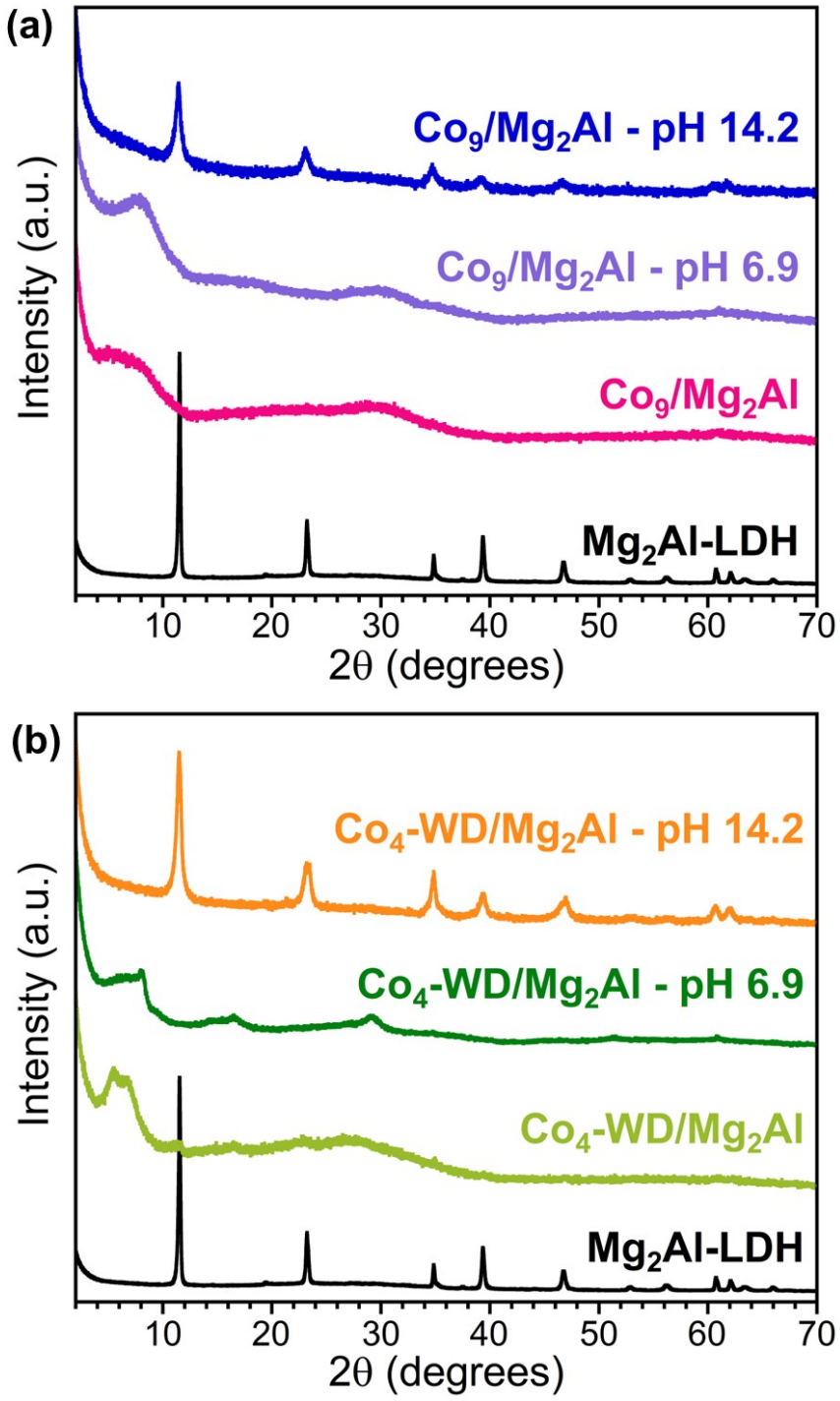

Fig. S6 Ex situ PXRD patterns of (a) Co_9/Mg_2Al and (b) Co_4-WD/Mg_2Al collected after the dispersing the nanocomposites in the working electrolytes for 72 h.

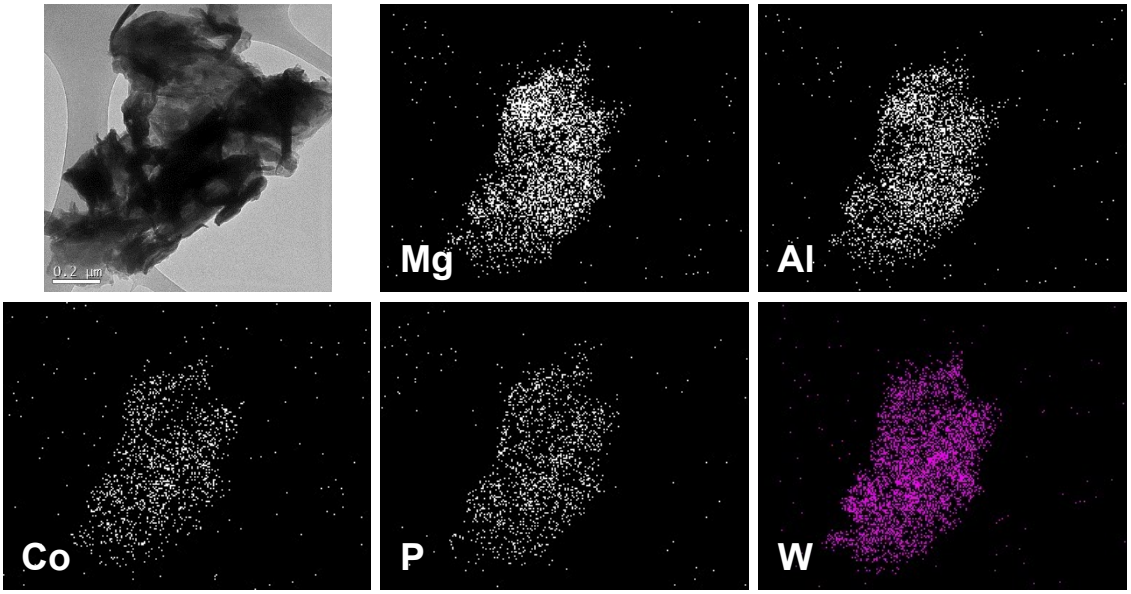

Fig. S7 Ex situ EDX mapping of the Co_9/Mg_2Al nanocomposite recovered after being immersed under stirring for 72 hours in the phosphate buffer at pH 6.9.

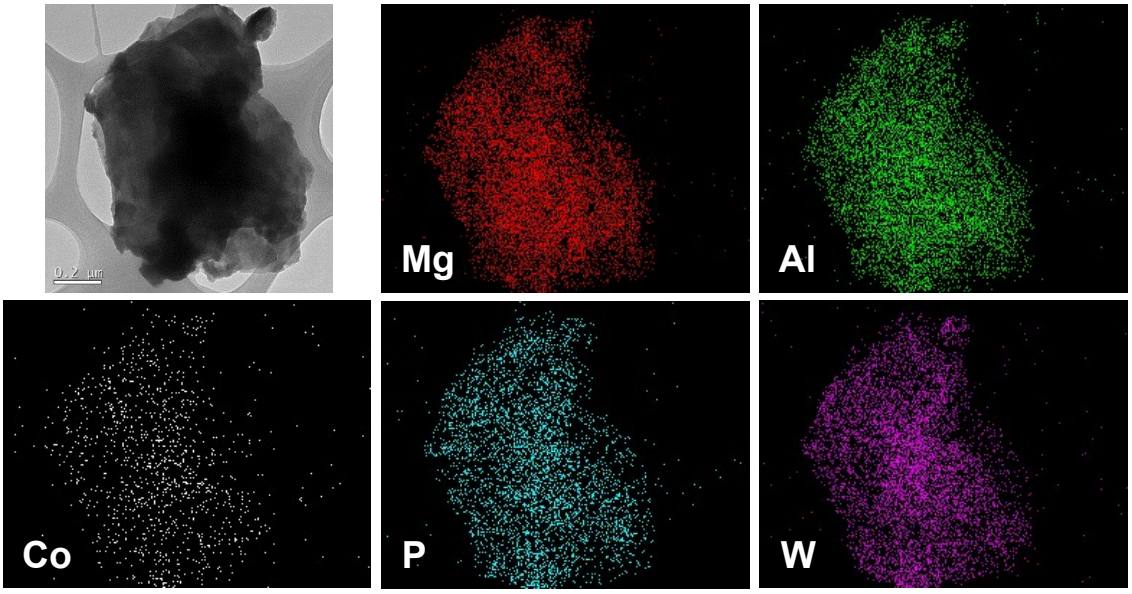

Fig. S8 Ex situ EDX mapping of the Co_4-WD/Mg_2Al nanocomposite recovered after being immersed under stirring for 72 hours in the phosphate buffer at pH 6.9.

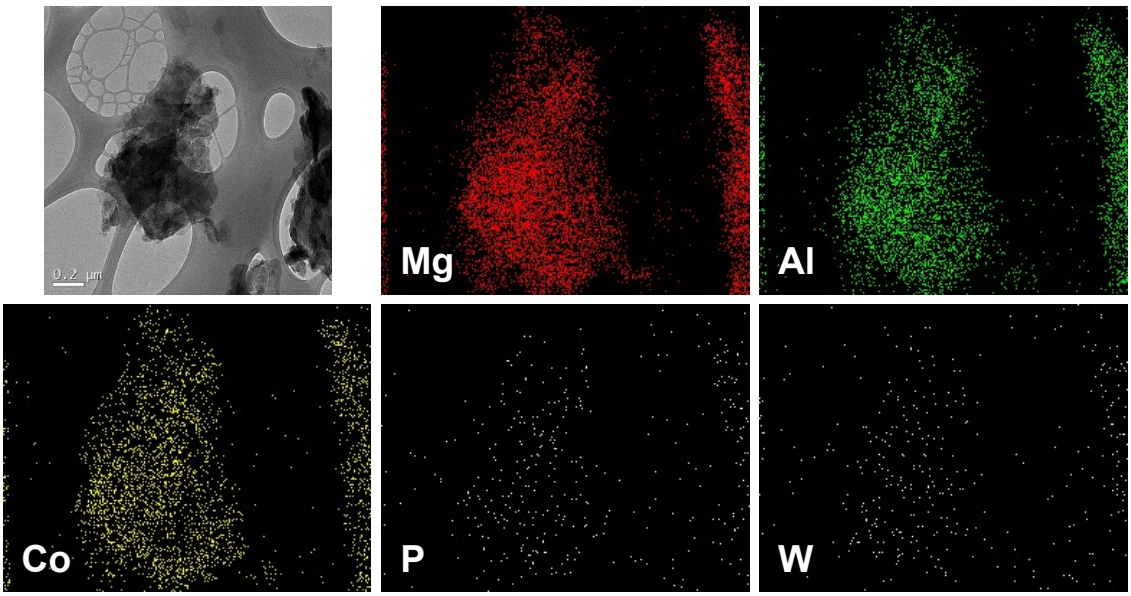

Fig. S9 Ex situ EDX mapping of the Co_9/Mg_2Al nanocomposite recovered after being immersed under stirring for 72 hours in KOH (1 M) at pH 14.2.

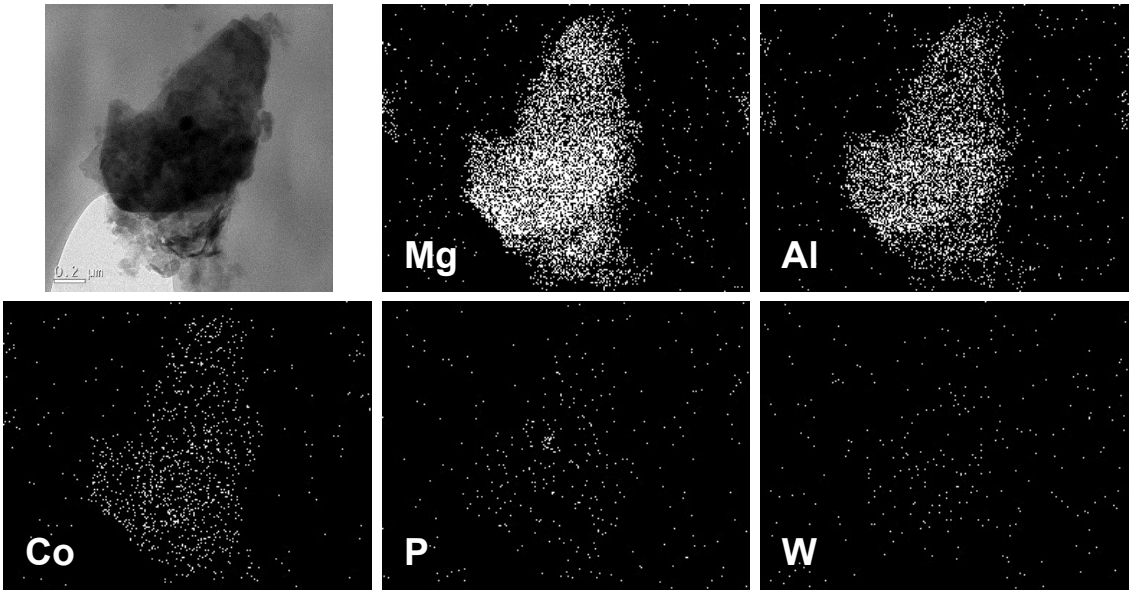

Fig. S10 Ex situ EDX mapping of the Co_4-WD/Mg_2Al nanocomposite recovered after being immersed under stirring for 72 hours in KOH (1 M) at pH 14.2.

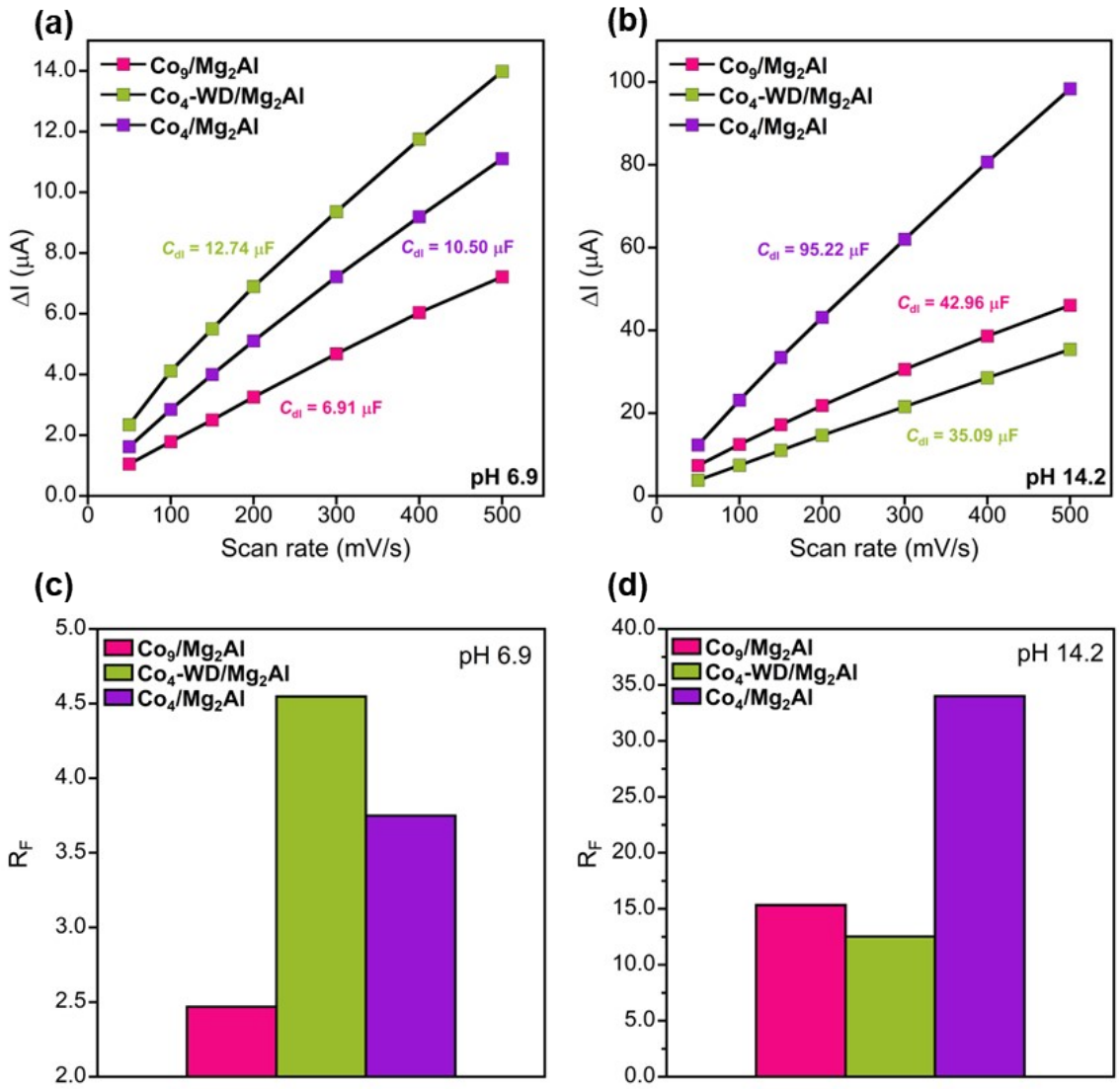

Fig. S11 ΔI (I_a-I_c) vs scan rate plot of the nanocomposites using (a) 0.1 M NaP_i buffer with 1M $NaNO_3$ as an electrolyte at pH 6.9 and (b) 1 M KOH electrolyte at pH 14.2., where the slope = 2 C_{dl}. Estimated roughness factor values of the nanocomposites at pH 6.9 (c) and at pH 14.2 (d).

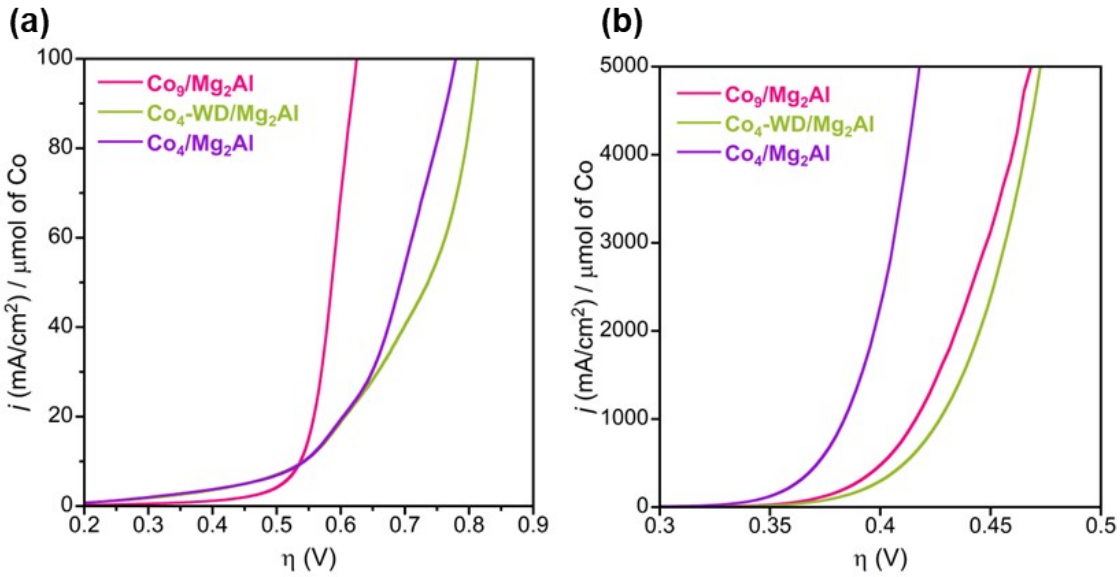

Fig. S12 Recorded linear sweep voltammetries using (a) 0.1 M NaP_i buffer with 1M $NaNO_3$ as an electrolyte at pH 6.9 and (b) 1 M KOH electrolyte at pH 14.2 normalised by the Co content in each fresh nanocomposite. At pH 6.9, the observed OER activity follows the same trend seen with the intrinsic activity (normalized by the RF), whereby the Co_9/Mg_2Al nanocomposite shows a better performance that the Co_4-WD/Mg_2Al and the Co_4/Mg_2Al nanocomposites. Furthermore, Co_4-WD/Mg_2Al and Co_4/Mg_2Al still show a very similar activity. These results suggest that under the present conditions, the OER activity of the POMs is influenced by the Co-oxo cluster of the POM rather than the nature of the supporting polyoxotungstate framework. Conversely, in alkaline conditions, where the Co-POMs seem to decompose leading to the formation of CoO_x species, the trend does not follow that observed with the intrinsic activity. In this situation, the Co_4/Mg_2Al nanocomposite delivers the best performance of the three examined materials, whereas Co_9/Mg_2Al and Co_4-WD/Mg_2Al display a similar activity. This data suggests that the polyoxotungstate framework has an observable influence on the formed CoO_x species, and therefore, on the resulting OER activity. For instance, Co_9/Mg_2Al shows the best activity when the data in normalized by the RF, whereas its activity is clearly reduced considering the Co content. Additionally, we obtained the opposite trend with Co_4/Mg_2Al and, in all cases Co_4-WD/Mg_2Al display the lowest activity. A possible explanation to this observation could arise from the number of Co centres in the formed CoO_x species that are available to interact with OH^- ions to evolve O_2, which in turn would agree with the obtained ECSA values. Therefore, the Co_9/Mg_2Al-derived CoO_x species may have a lower number of Co active centres than the Co_4/Mg_2Al-derived CoO_x species, although these Co active centres should possess a higher OER activity.

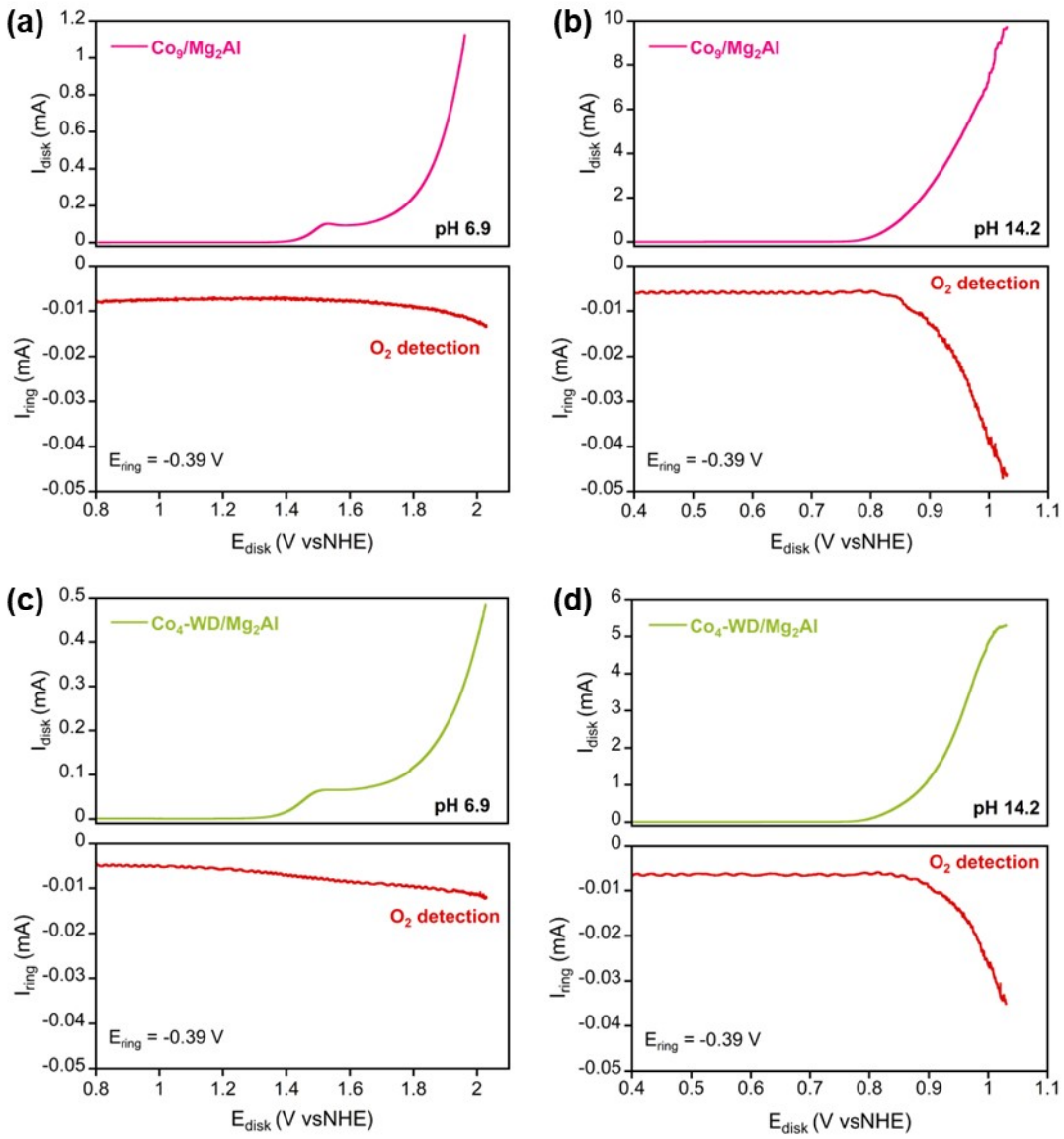

Fig. S13 Rotating ring disk electrode (RRDE) experiments using either Co_9/Mg_2Al (a-b) or Co_4-WD/Mg_2Al (c-d) showing the detection of O_2. The experiments were performed in bipotentiostat mode using a single cell under Ar atmosphere employing (a,c) 0.1 M NaP_i buffer with 1M $NaNO_3$ as an electrolyte at pH 6.9 and (b,d) 1 M KOH electrolyte at pH 14.2. The applied potential at the glassy carbon disk was scanned to positive values with a scan rate of 1 mV/s, whereas a constant applied potential of -0.39 V was held on the Pt ring to detect the O_2 evolved (red lines). The rotation speed of the RRDE electrode was 700 rpm.

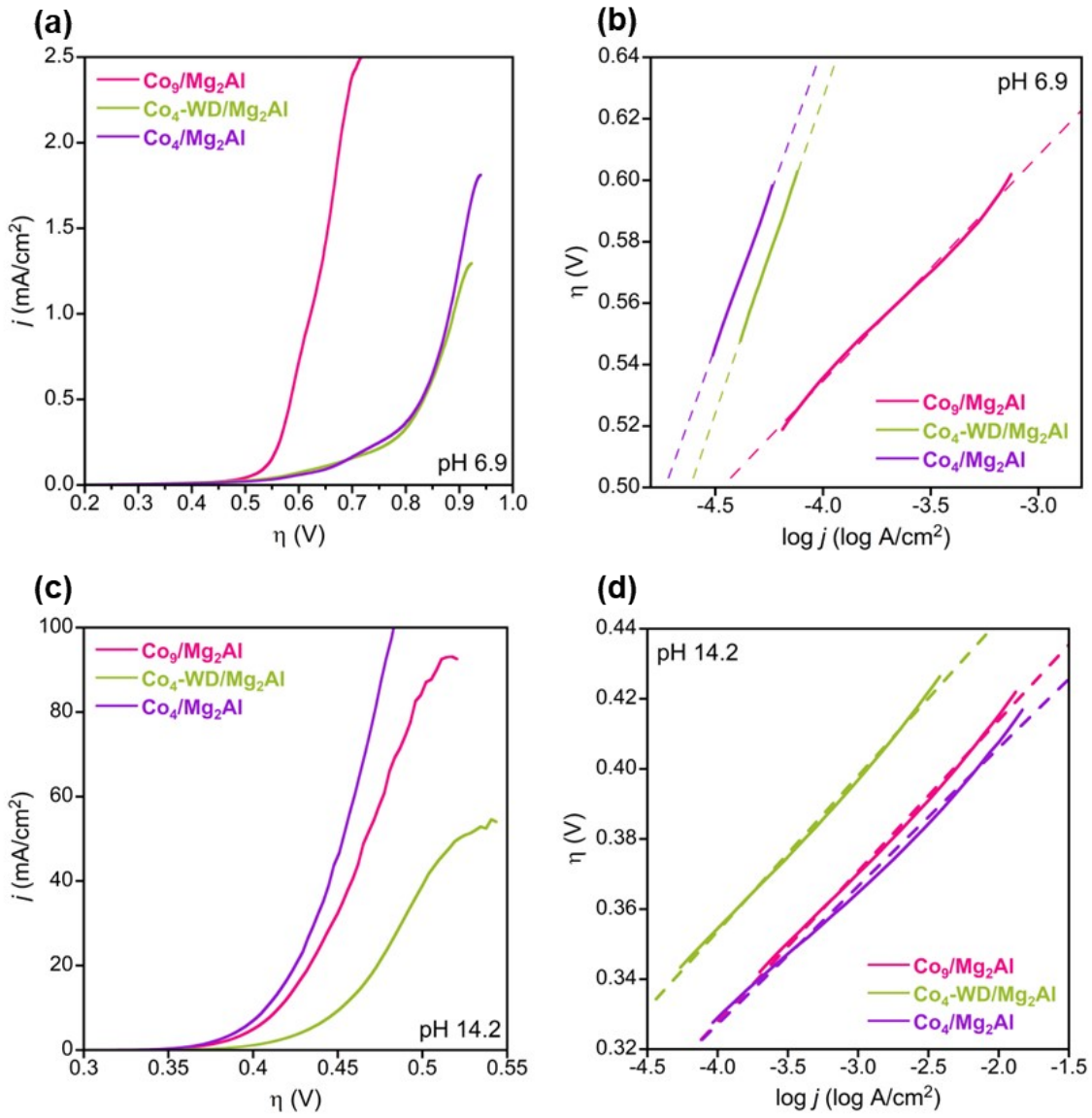

Fig. S14 Recorded linear sweep voltammetry and Tafel plot of the nanocomposites using (a-b) 0.1 M NaP_i buffer with 1M $NaNO_3$ as an electrolyte at pH 6.9 and (c-d) 1 M KOH electrolyte at pH 14.2.

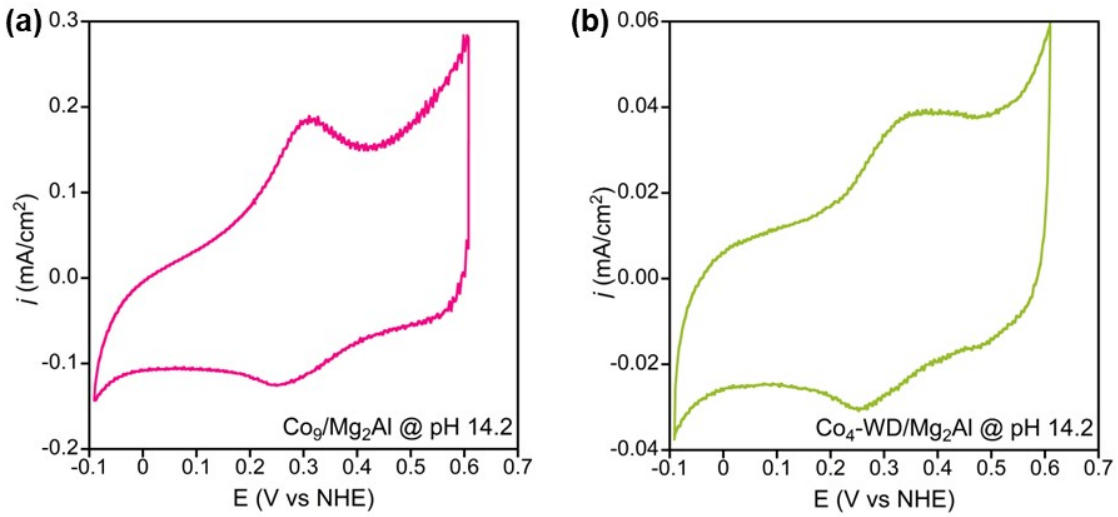

Fig. S15 Cyclic voltammogram of (a) Co_9/Mg_2Al and (b) Co_4-WD/Mg_2Al nanocomposites showing the appearance of a new redox pair during the preconditioning cycles performed using the 1 M KOH electrolyte at pH 14.2. The redox pairs are assigned to the Co(II)/Co(III) pair originated from the intercalated CoO_x formed due to the Co(II) ions leached from the Co-POM structure, highlighting their low stability in alkaline media.

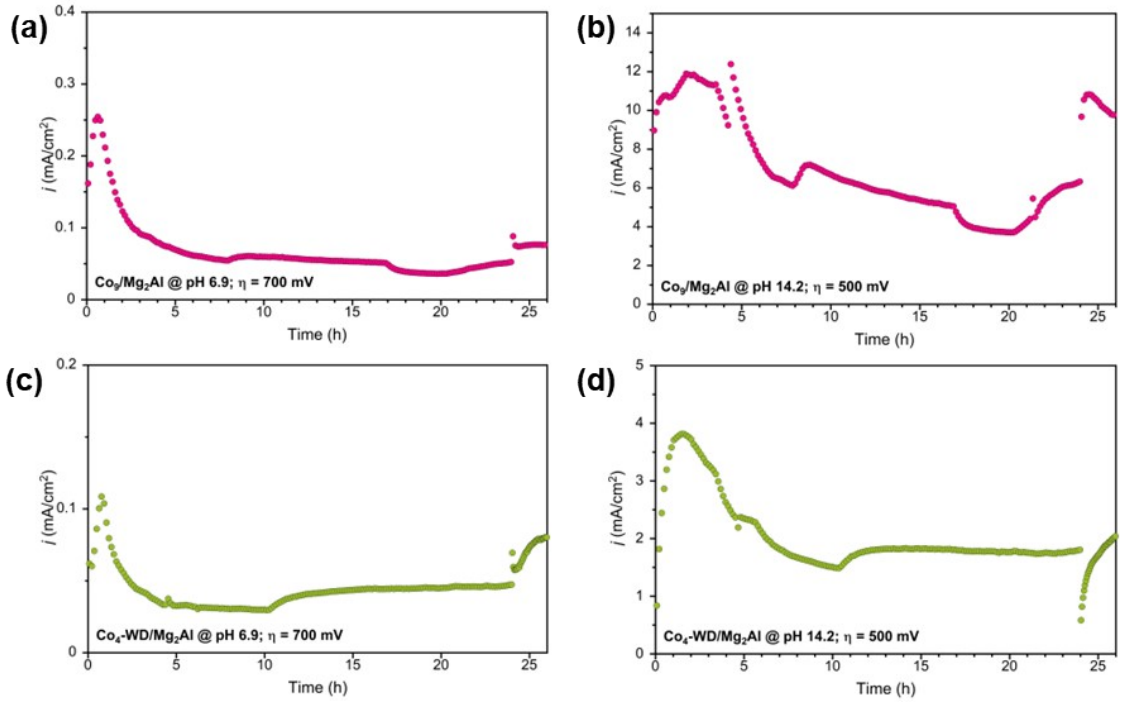

Fig. S16 Chronoamperometric measurements of Co_9/Mg_2Al and Co_4-WD/Mg_2Al nanocomposites using (a-c) 0.1 M NaP_i buffer with 1M $NaNO_3$ as an electrolyte at pH 6.9 and (b-d) 1 M KOH electrolyte at pH 14.2. The decrease in the current density after 24 hours is assigned to the trapping of oxygen bubbles on the surface of the electrodes. After this time, the oxygen bubbles were removed from the electrodes, and the experiments were repeated for two extra hours mostly recovering the initial current densities. Note that the prepared Nafion inks were not reformulated for these experiments since we are not seeking performance but to study the stability of the nanocomposites under these conditions.

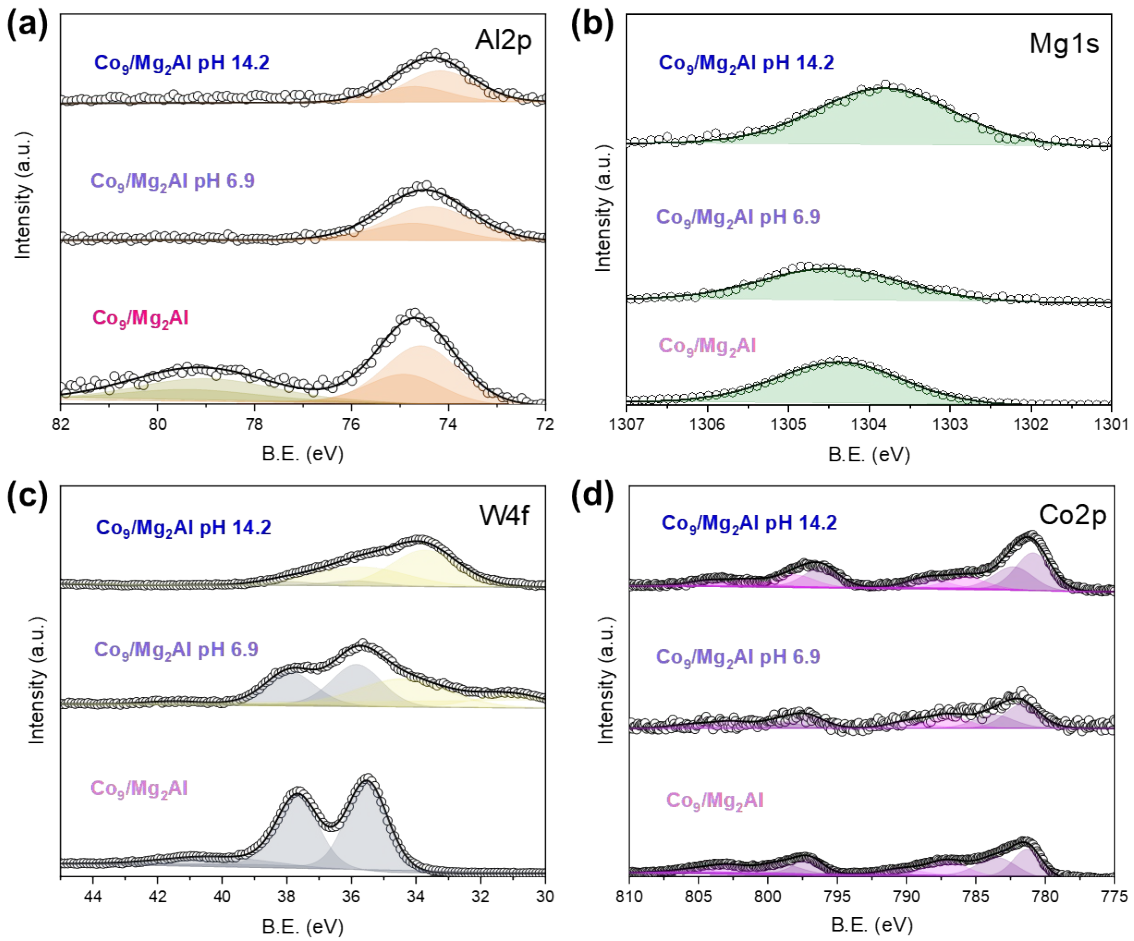

Fig. S17 XPS data comparing the fresh Co_9/Mg_2Al nanocomposite to those of the postcatalytic samples after 24 hours of chronoamperometric measurements. The XPS were recorded directly on the surface of the modified carbon paper working electrodes. Note that the Nafion polymer shows a strong overlap with the W 4f edge, shown in yellow in (c).[3]

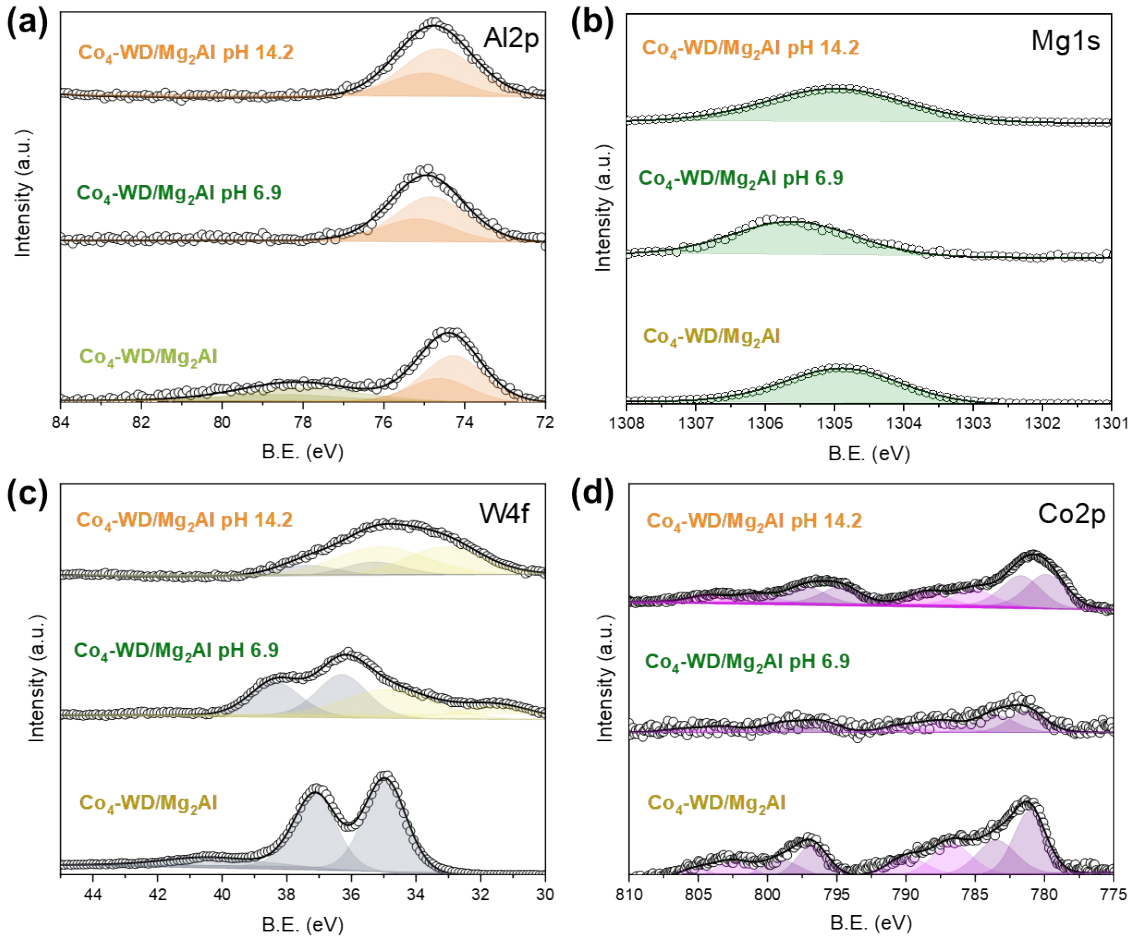

Fig. S18 XPS data comparing the fresh Co_4-WD/Mg_2Al nanocomposite to those of the postcatalytic samples after 24 hours of chronoamperometric measurements. The XPS were recorded directly on the surface of the modified carbon paper working electrodes. Note that the Nafion polymer shows a strong overlap with the W 4f edge, shown in yellow in (c).[3]

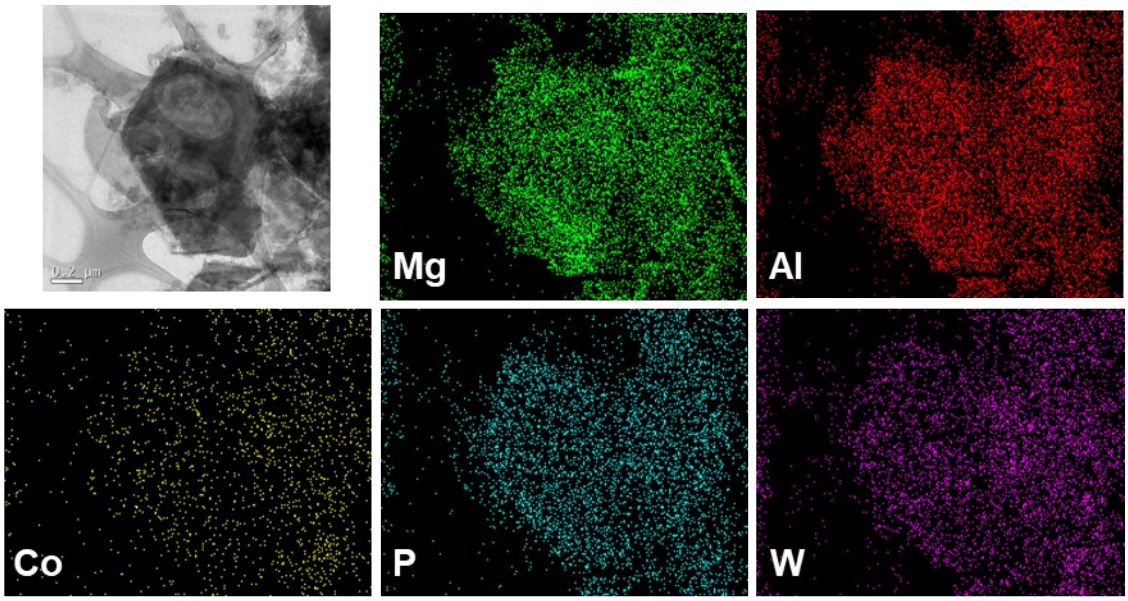

Fig. S19 TEM image and EDX mapping of the Co_9/Mg_2Al nanocomposite recovered after 24 hours of chronoamperometric measurements using the 0.1 M NaP_i buffer at pH 6.9 with 1M $NaNO_3$ as an electrolyte. The W:Co ratio found is 2.87 (expected W:Co ratio = 3), which suggests that the Co_9 is stable under working conditions. Note that the intercalation of phosphates from the NaP_i buffer in the interlayer space of the LDH during the measurements precludes the calculation of the P:Co ratio.

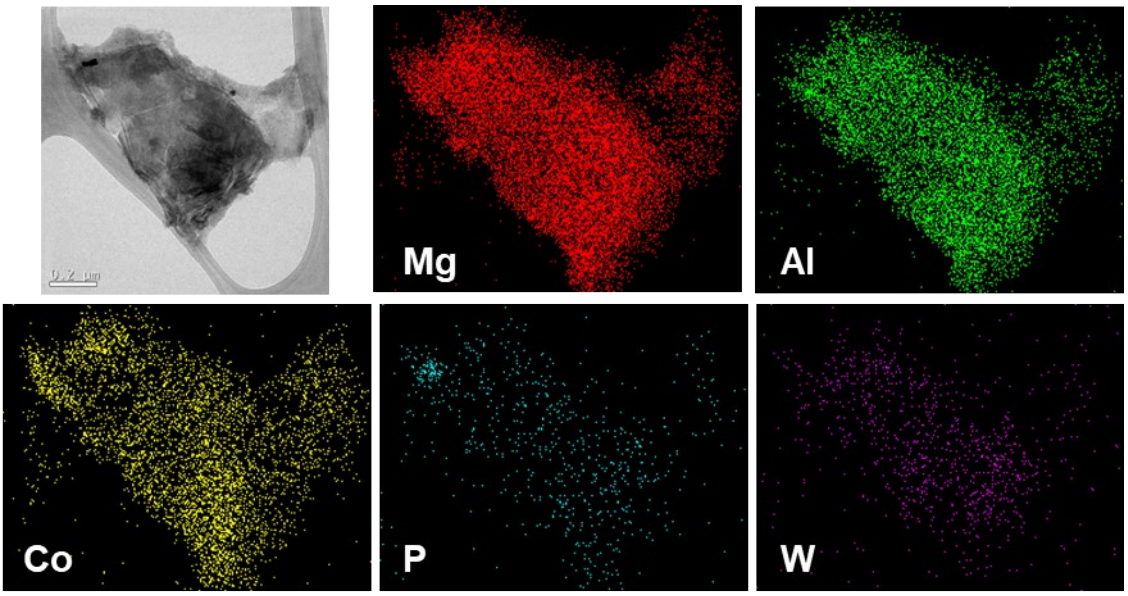

Fig. S20 TEM image and EDX mapping of the Co_9/Mg_2Al nanocomposite recovered after 24 hours of chronoamperometric measurements using the 1 M KOH electrolyte at pH 14.2. The W:Co ratio found is 0.26 (expected W:Co ratio = 3) and the P:Co ratio found is 0.04 (expected P:Co ratio = 0.56). The high decrease in W and P content in the postcatalytic nanocomposite suggests that the Co_9 decomposes under such working conditions leading to the formation of CoO_x species, as suggested by XPS and electrochemical analysis.

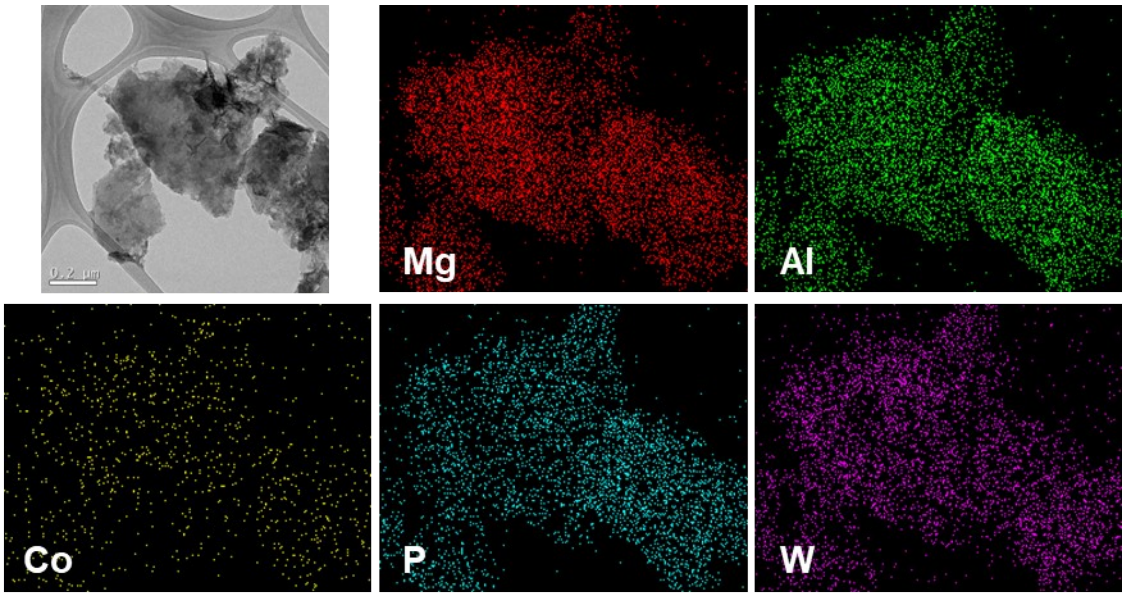

Fig. S21 TEM image and EDX mapping of the Co_4-WD/Mg_2Al nanocomposite recovered after 24 hours of chronoamperometric measurements using the 0.1 M NaP_i buffer at pH 6.9 with 1M $NaNO_3$ as an electrolyte. The W:Co ratio found is 6.74 (expected W:Co ratio = 7.5), which suggests that the Co_4-WD is stable under working conditions. Note that the intercalation of phosphates from the NaP_i buffer in the interlayer space of the LDH during the measurements precludes the calculation of the P:Co ratio.

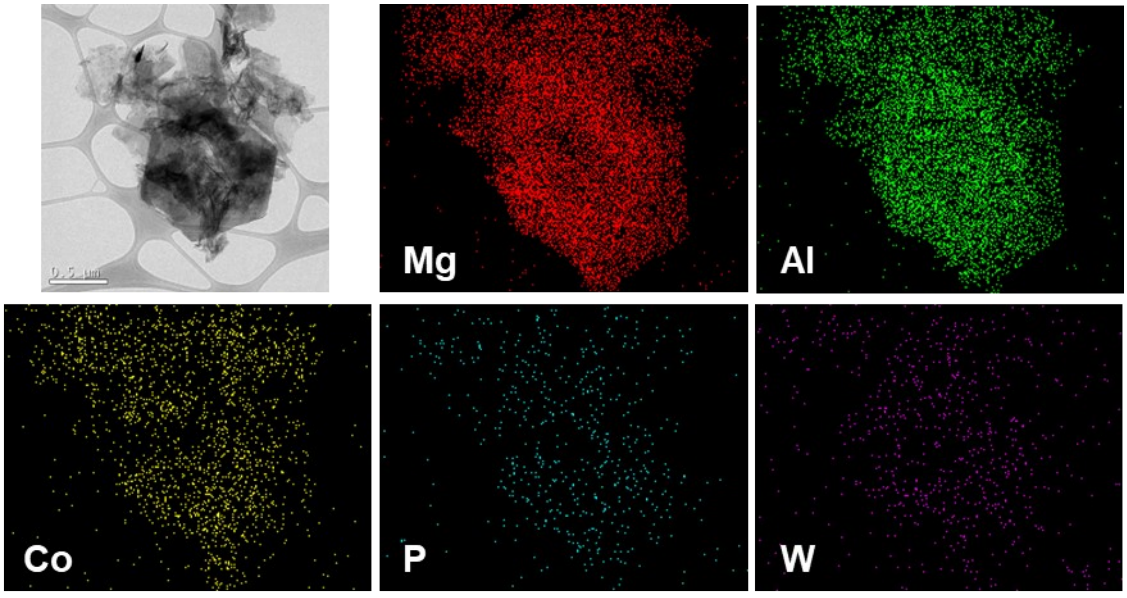

Fig. S22 TEM image and EDX mapping of the Co_4-WD/Mg_2Al nanocomposite recovered after 24 hours of chronoamperometric measurements using the 1 M KOH electrolyte at pH 14.2. The W:Co ratio found is 0.44 (expected W:Co ratio = 7.5) and the P:Co ratio found is 0.04 (expected P:Co ratio = 0.50). The high decrease in W and P content in the postcatalytic nanocomposite suggests that the Co_4-WD decomposes under such working conditions leading to the formation of CoO_x species, as suggested by XPS and electrochemical analysis.

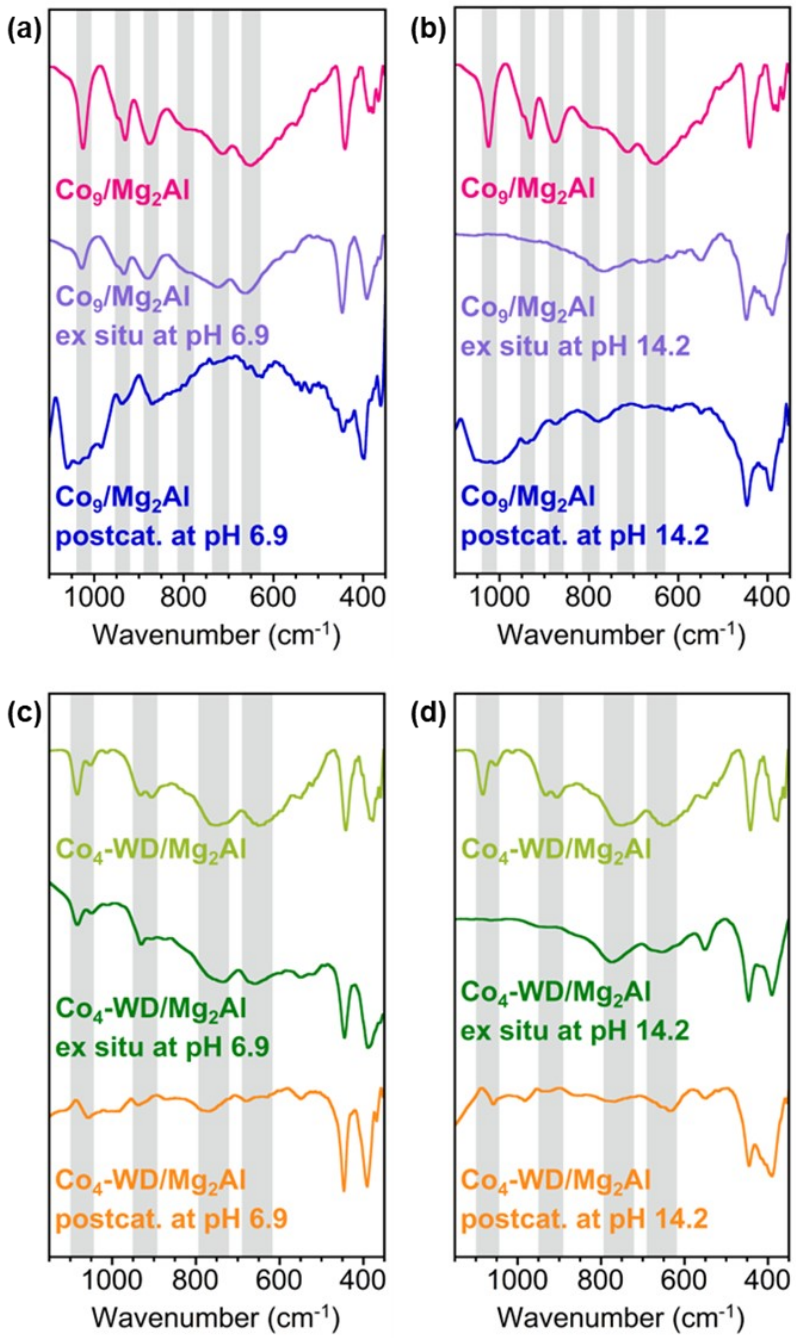

Fig. S23 FT-IR spectra of (a-b) Co_9/Mg_2Al and (c-d) Co_4-WD/Mg_2Al comparing the fresh materials with those recovered after immersion in the electrolytes for 72 hours (ex situ) and with the recovered (postcatalytic) materials after 24 hours of chronoamperometric experiments. The data suggest that Co-POMs are stable in close-to-neutral media and suffer structural transformations in alkali conditions. Ex situ data unequivocally show the disappearance of the main POM features in alkaline media. On the other hand, the recovered postcatalytic materials still show some bands that could be associated with the POM structure, although these are of less intensity than the fresh materials. Considering all the data together, we assign these bands to trapped tungstate and phosphate species within the CoO_x matrix formed from Co-POM decomposition. Nevertheless, X-ray absorption measurements would be required to unambiguously identify the nature of the species formed in alkali media, which are beyond the scope of the present work.

5) References:

1 J. R. Galán-Mascarós, C. J. Gómez-Garcia, J. J. Borrás-Almenar and E. Coronado, *Adv. Mater.*, 1994, **6**, 221–223.

2 R. G. Finke, M. W. Droege and P. J. Domaille, *Inorg. Chem.*, 1987, **26**, 3886–3896.

3 J. Soriano-López, J. Quirós-Huerta, Á. Seijas-Da Silva, R. Torres-Cavanillas, E. Andres-Garcia, G. Abellán and E. Coronado, *Inorg. Chem.*, 2025, **64**, 3242–3255.

4 C. C. L. McCrory, S. Jung, J. C. Peters and T. F. Jaramillo, *J. Am. Chem. Soc.*, 2013, **135**, 16977–16987.